

Article

Influence of Road Patterns on PM_{2.5} Concentrations and the Available Solutions: The Case of Beijing City, China

Fang Wang *, Yaoyao Peng and Chunyan Jiang

Sino-German Joint Laboratory on Urbanization and Locality Research (UAL), College of Architecture and Landscape Architecture, Peking University, Beijing 100871, China; pengyy@pku.edu.cn (Y.P.); Jchunyan@pku.edu.cn (C.J.)

* Correspondence: wfphd@pku.edu.cn; Tel./Fax: +86-10-6275-9003

Academic Editor: Tan Yigitcanlar

Received: 22 November 2016; Accepted: 25 January 2017; Published: 7 February 2017

Abstract: With the increase in urbanization and energy consumption, PM_{2.5} has become a major pollutant. This paper investigates the impact of road patterns on PM_{2.5} pollution in Beijing, focusing on two questions: Do road patterns significantly affect PM_{2.5} concentrations? How do road patterns affect PM_{2.5} concentrations? A land-use regression model (LUR model) is used to quantify the associations between PM_{2.5} concentrations, and road patterns, land-use patterns, and population density. Then, in the condition of excluding other factors closely correlated to PM_{2.5} concentrations, based on the results of the regression model, further research is conducted to explore the relationship between PM_{2.5} concentrations and the types, densities, and layouts of road networks, through the controlling variables method. The results are as follows: (1) the regression coefficient of road patterns is significantly higher than the water area, population density, and transport facilities, indicating that road patterns have an obvious influence on PM_{2.5} concentrations; (2) under the same traffic carrying capacity, the layout of “a tight network of streets and small blocks” is superior to that of “a sparse network of streets and big blocks”; (3) the grade proportion of urban roads impacts the road patterns’ rationality, and a high percentage of branch roads and secondary roads could decrease PM_{2.5} concentrations. These findings could provide a reference for the improvement of the traffic structure and air quality of Beijing.

Keywords: road patterns; land-use; air pollution; sustainable city; LUR model

1. Introduction

With rapid urbanization, high population density and heavy traffic exacerbate the air pollution arising from a traditional extensive economy. The frequent occurrence of PM_{2.5} pollution offers a warning against rapid urban development, which also underscores the importance of constructing a scientific and reasonable city structure. Previous studies have shown that PM_{2.5} concentrations in different urban spaces are variable [1,2], as they are affected by the urban spatial pattern [3], land development intensity [4,5], public green spaces [6], road grades, and traffic [7]. For example, Chan et al. (2001) [8] found that the concentration of PM_{2.5} in an urban industrial district, a residential area, and a business district of Hong Kong, was 77.6, 107.0, and 88.5 µg/m³, respectively. Li et al. (2012) [9] noted that the annual concentration of PM_{2.5} in a green space was lower than that in bare land.

Among these factors, motor vehicles have become important sources of fine particulate pollution, contributing between 25% and 35% of direct PM_{2.5} emissions [10,11], which are the dominant source of air pollution in most urban cities [12,13]. Meanwhile, “Particulate matter (PM) pollutants are

currently of high interest, because medical findings indicate that adverse health effects are caused by aerosol particles in the ultrafine (<100 nm diameter) size range that are associated with traffic" [14]. The previous research on vehicle emissions of particulates has mainly focused on their black carbon or particle number concentrations, especially for diesel vehicles, which require high equipment and technology [15,16]. Compared to light-duty gasoline vehicles, primary PM_{2.5} emissions from heavy-duty diesel vehicles can be between one and two orders of magnitude higher [14]. As a result, diesel vehicles have been gradually controlled, and gasoline vehicles occupy 84.7% of the total number of motor vehicles in China [17]. With the renewal of vehicle technology, gasoline direct injection (GDI) technology has been widely used, which is different from traditional port fuel injection (PFI) technology. GDI has a good fuel economy and an emission reduction effect of CO₂, but has caused the significant increase in particle emissions [18]. Meanwhile, due to the constraints of technology and difficulties in data acquisition to capture the concentrations of black carbon or other particulates, our research uses PM_{2.5} as the indicator for vehicle particle emissions.

Many studies have explored PM_{2.5} emissions from on-road vehicles [19–21], and the effect of exposure to traffic-related PM_{2.5} on human health [22–24]. Panis et al. (2011) [25] observed that the effects of specific speed reduction schemes on PM emissions from trucks are ambiguous. Xu et al. (2016) [26] examined the commuters' exposure to PM_{2.5} in the Shanghai metro system and found that the metro in-carriage PM_{2.5} concentrations were significantly affected by the ventilation systems, out-carriage PM_{2.5} concentrations, and the passenger numbers. However, few studies have investigated the relationship between PM_{2.5} and the structure of road networks. As an important component of sustainable cities, reasonable road layouts would not only ease traffic congestion [27] and save energy, but also reduce the impacts on the environment [28]. Additionally, it has been reported that PM_{2.5} concentrations near busy roads could be 30% higher than the background levels [29]. Therefore, further research is still necessary to understand the requirements for a more sustainable and environmentally-friendly road network.

The objective of this paper is to assess the effect of road networks on PM_{2.5} pollution, which mainly focuses on two questions: Do road patterns significantly affect PM_{2.5} concentrations? How do road patterns affect PM_{2.5} concentrations? During the study, PM_{2.5} concentrations were the dependent variable, and road patterns, land-use, and population density were the independent variables, through which a land-use regression model (LUR model) was obtained. By comparing the regression coefficient of road patterns with other factors, the extent of its influence can be determined. Then, by referring to the variable-control approach and excluding the influence of other irrelevant variables, the grades, densities, and layouts of road patterns, can be used to analyze their relationship with the surrounding PM_{2.5} concentrations.

2. Materials and Methods

2.1. Study Area

Beijing (115.7°E–117.4°E, 39.4°N–41.6°N), the capital of China, is located in the North China Plain, and is adjacent to a semi-desert area. At an average elevation of 43.5 m, Beijing is surrounded by highlands on three sides. The elevation of the mountain area reaches up to 1500 m above sea level, which is unfavorable for pollution dispersion. Low forest coverage (14.85%) further exacerbates the problem of air pollution. Beijing's climate is a typical continental monsoon climate, characterized by hot and rainy summers, and cold and dry winters. The average annual precipitation has been less than 450 mm over the last decade, with 80% of the rainfall being mainly concentrated in the summer. With the development of the city, and under the influence of its surroundings, air pollution in Beijing is becoming increasingly serious, with a higher concentration of PM_{2.5} in the southern part, than the northern part of Beijing. Considering the major differences between urban areas and suburbs, as well as the distribution characteristics of the air-quality monitoring sites, this paper takes the central zone of Beijing as the study area, including the Dongcheng District, Xicheng District, Chaoyang District,

Haidian District, Fengtai District, and Shijingshan District, which together cover 8% of Beijing's land area, 60% of the region's population, and 70% of the region's industries. The traffic index of the central zone of Beijing is around 5.5, which is little higher than the Beijing average traffic index of 5.1, meaning that parts of the ring and main roads are congested.

2.2. LUR Model

Approaches that have been developed to simulate the distribution of the concentration of air pollutants usually include geostatistical interpolation [30], land-use regression [31], dispersion [32], and hybrid [33] models. "Dispersion models use information on emissions, source characteristics, chemical and physical properties of the pollutants, topography, and meteorology to model the transport and transformation of gaseous or particulate pollutants through the atmosphere to predict, e.g., ground level concentrations" [34]. Also, it is expensive and difficult to obtain the high-precision data of pollutant sources and meteorology, which then has to be initialized and parameterized. Moreover, the interpolation method is only based on the monitoring of data, which means that it is hard to indicate the spatial variation of pollutant concentration on a small scale [35]. Compared with these methods, land-use regression (LUR) has been widely used, and has rapidly become an important approach for predicting long-term average pollutant concentration at an intra-urban scale [36]. Also, it is a promising approach for predicting ambient air pollutant concentrations at high spatial resolution [37,38], as it has a low requirement for the categories of the data, and the model is simple to construct. With less accurate exposure-estimating methodologies, such as those based on ambient city-wide monitoring or distance to road calculations, an increased exposure measurement error may bias the models toward null [39]. Moreover, the concentration of ambient pollution is usually used as a dependent variable, while the surrounding land-use, transportation, and population density are extracted using geographic information systems (GIS) and are included in a regression equation as predictor variables [40,41]. The LUR model has been applied in more than nine countries and 14 cities across Europe (e.g., [42,43]) and North America (e.g., [44,45]). European and North American LUR models yielded a predictive capacity (as R^2) ranging from 35% to 94% for $PM_{2.5}$ [36].

The keys to the success of the LUR model are as follows: (1) The selection of variables: the specific modeling usually requires three to five variable categories, and some of the most widely used include land-use, traffic emission, meteorology, population density, distribution of emission source, altitude, and so on; (2) Removing and selecting the variables: three principles should be considered, which are that variables are not significantly correlated with X_i , they meet the t -statistics values, and the R^2 value is not less than 1%; (3) The choice of the buffer radius of the air-quality monitoring site: the buffer radius is closely related to the spatial precision and the research scale. Under normal conditions, the maximum buffer radius of land-use and population density could be up to 5000 m, and the maximum buffer radius of the road is relatively small [46].

The LUR model-building steps usually include the following: (1) Calculating the correlation between the variables and $PM_{2.5}$ concentrations, and then ranking all of the variables by the absolute value of their correlation with $PM_{2.5}$ concentrations; (2) Identifying the highest-ranking variable in each subcategory (Subcategory is a subdivision that has common differentiating characteristics within a larger category); (3) Eliminating other variables in each subcategory that are significantly correlated to the most highly ranked variable; (4) Entering the rest of the variables into a database for stepwise linear regression; (5) Removing any variables that have insignificant t -statistics values from the available pool; and (6) Repeating steps four and five to converge data, removing any variable that contributes to less than 1% of the R^2 value, for a parsimonious final model [37]. The general regression equation of the LUR model is as follows:

$$c = a_0 + \sum a_i \cdot X_i + \varepsilon_i, i = 1, 2, 3, \dots, n \quad (1)$$

In Equation (1), c is the concentration of $PM_{2.5}$; a_i ($i = 0, 1, 2, \dots, n$) are regression coefficients; X_i ($i = 0, 1, 2, \dots, n$) are independent variables; ε_i is the random error.

2.3. Data Collection

2.3.1. Monitoring Sites

The data on $PM_{2.5}$ concentrations were collected from 35 air-quality monitoring sites in Beijing, which can be sorted into five categories: 12 urban background sites, 11 suburban background sites, five curbside sites, six surrounding regional sites, and one reference site (Figure 1). The reference site is included with the aim of reflecting the level of air quality in urban areas that not affected by local pollution. Moreover, these real-time monitoring data are posted online by the Beijing Municipal Environmental Monitoring Center in *Beijing Air Quality Real-time Broadcasting* (<http://zx.bjmemc.com.cn/>). Among these monitoring sites, the five curbside sites are located along main roads and are directly exposed to traffic emissions, while the 12 urban background sites are located far from the roads. These two types of sites are completely located within the study area. The $PM_{2.5}$ data used in this paper are the annual average concentrations of both curbside sites and urban background sites in 2015.

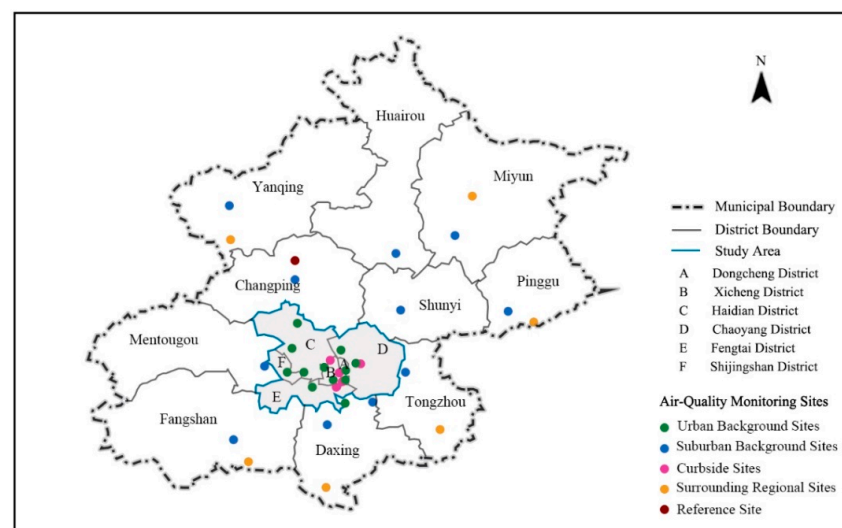


Figure 1. The distribution of air-quality monitoring sites in Beijing (Source: by Authors).

2.3.2. Road Traffic Data

The differences in traffic monitoring programs in urban areas result in variable types of traffic indicators. If cars and trucks are systematically enumerated, then variables reflecting traffic intensity can be generated. However, if traffic counts do not exist, then road classifications can be used as a surrogate, because road classification can reflect traffic volumes at a certain level. The higher the road level is, the larger the traffic flows are. Henderson et al. attempted to assess whether a similar LUR model could be obtained from the two different sets of traffic variables—traffic volume and road patterns. All of these results suggest that models built with road length and vehicle density metrics, are equally able to explain the variability in pollutant concentrations. This finding confirms that valuable LUR models can be developed in the absence of traffic count data, which are unreliable or nonexistent in many areas [37]. Many other scholars have also used road patterns to build LUR models [47,48]. Since it is difficult to collect the traffic flow data in Beijing, road classifications were selected in this study. During further research, roads were divided into five classes, including expressways, fast roads, arterial roads, secondary roads, and branch roads (Figure 2). The corresponding data come from the *Master Planning of Beijing (2004–2020)* [49] and *Beijing Traffic Tourism Map (2015)* [50].

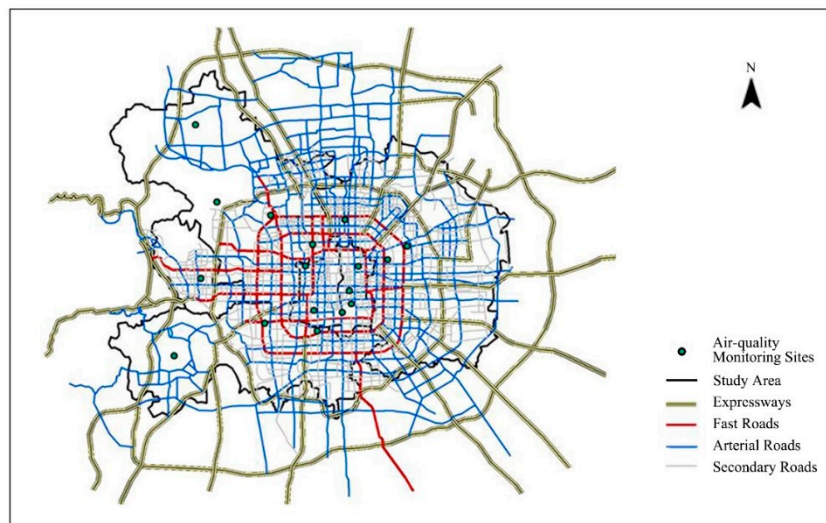


Figure 2. The road network of the study area (2015). The branch roads were removed from display as they were dense (Source: Basic data from Beijing Municipal Institute of City Planning & Design and Google Earth, modified by authors).

2.3.3. Land-Use Data

The land-use map of Beijing in 2014 was compiled by the Beijing Municipal Institute of City Planning & Design, which was then combined with the satellite imagery of Google Earth to obtain the land-use map of the study area in 2015. According to the *Code for classification of urban land-use and planning standards of development land*, and its positive and negative influences on $PM_{2.5}$, land is divided into five types, including *water*, *vegetation*, *transportation land*, *other developed land*, and *other non-developed land* (Figure 3, Table 1). It is particularly worth mentioning here that, because the impact of traffic on $PM_{2.5}$ concentrations is measured by the lengths of different roads, the land represented by road is not included in *transportation land*.

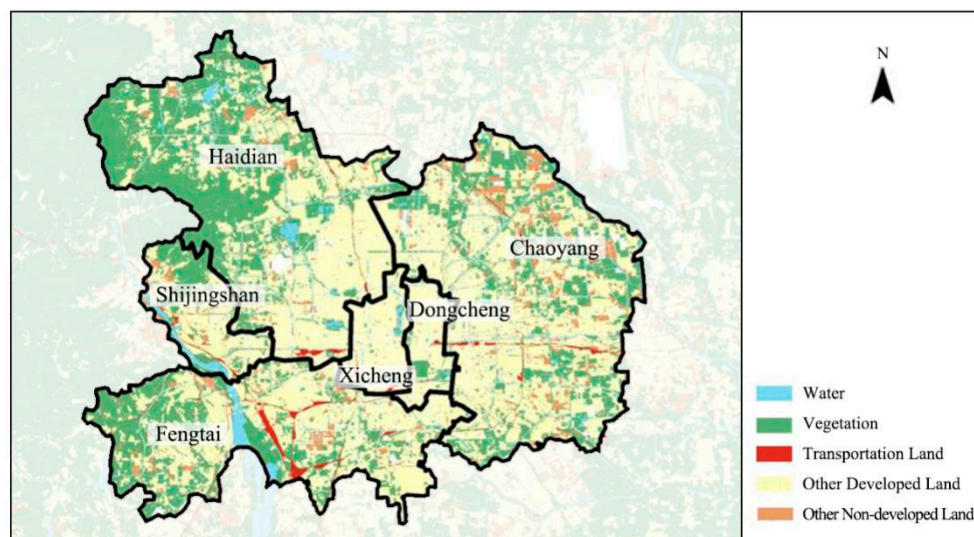


Figure 3. The land-use map of the study area (2015) (Source: Basic data from Beijing Municipal Institute of City Planning & Design and Google Earth, modified by authors).

Table 1. Land-use classification.

Land Type	Details
Water	Rivers, lakes, reservoirs, channels, ponds, wetlands, etc.
Vegetation	Urban green land, cultivated and woody land (dry lands, orchards, shrub lands, artificial grasslands, paddy fields, forest lands, irrigated lands, etc.).
Transportation land	Transportation hub lands (railway stations, highway bus stations, port passenger terminals, public transport hubs, etc.), parking lots, traffic squares, etc.
Other developed land	Residential lands, commercial lands, industrial lands, villages, lands for mining, scenic spots, etc.
Other non-developed land	Swamps, bare lands, other grasses, etc.

2.3.4. Population Data

With a dense population, the study area supports approximately 60% of Beijing's permanent residents. Because this population could reflect the residential energy consumption, population data are also considered as a factor affecting the air quality [51]. The population data were taken from the *Beijing Statistical Yearbook 2015* (Table 2) [52].

Table 2. Population data of the study area.

Area	Land Area (km ²)	Population (Million)	Population Density (No. of Persons/km ²)
Dongcheng District	41.86	91.1	21,763
Xicheng District	50.53	130.2	25,767
Chaoyang District	455.08	392.2	8618
Fengtai District	305.80	230.0	7521
Shijingshan District	84.32	65.0	7709
Haidian District	430.73	367.8	8539
Total	16,410.54	2151.6	1311

Source: Beijing Statistical Yearbook 2015 [52].

3. Results

3.1. Air Quality in Beijing

Figure 4 shows the air quality of Beijing over the last three years. Spring runs from March to May, summer from June to August, autumn from September to November, and winter from December to February. The heating season in Beijing is always between November and March.

From the perspective of annual variation, the air quality of Beijing has improved in fluctuation in recent years (annual mean concentrations of PM_{2.5} for 2013, 2014, and 2015 were 98, 89, and 86 µg/m³, respectively). However, this air quality continues to be far below both the international standard (10 µg/m³), and the national first level standard (35 µg/m³). From the perspective of seasonal variation, PM_{2.5} pollution varies largely with the season, with the highest pollution occurring in winter, and the least pollution occurring in summer and autumn. From the perspective of monthly variation, PM_{2.5} concentrations fluctuate greatly throughout the year. The peaks in 2013 and 2014 appeared in February, and can be seen in December during 2015, while the troughs during 2013 to 2015 were in August. Previous studies show that the major reason for the frequent PM_{2.5} pollution in winter is the coal-fired heating during that time, in both Beijing and the surrounding areas [53]. Moreover, the lighting of fireworks during the spring festival also results in poor air quality.

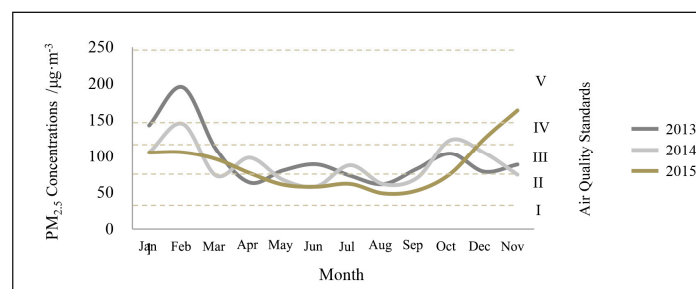


Figure 4. Monthly mean concentrations of $PM_{2.5}$ in the study area (2013–2015). The latest China National Ambient Air Quality Standards for $PM_{2.5}$ are: I. Excellent, 0–35 $\mu\text{g}/\text{m}^3$; II. Good, 35–75 $\mu\text{g}/\text{m}^3$; III. Slight pollution, 75–115 $\mu\text{g}/\text{m}^3$; IV. Moderate pollution, 115–150 $\mu\text{g}/\text{m}^3$; V. Heavy pollution, 150–250 $\mu\text{g}/\text{m}^3$; VI. Extremely heavy pollution, above 250 $\mu\text{g}/\text{m}^3$ (Source: by Authors).

According to the records (Figure 5), $PM_{2.5}$ concentrations around curbside monitoring sites (the annual average concentrations of $PM_{2.5}$ for 2013, 2014, and 2015 were 103, 96, and 91 $\mu\text{g}/\text{m}^3$, respectively) were higher than those around the urban background sites (the annual average concentrations of $PM_{2.5}$ for 2013, 2014, and 2015 were 95, 86, and 83 $\mu\text{g}/\text{m}^3$, respectively), due to road dust and emissions from vehicles. The standard deviations of $PM_{2.5}$ concentrations during each month were high, indicating that $PM_{2.5}$ pollution might suffer a significant volatility in a short period of time, as a result of Beijing's peculiar geographical locations, meteorological conditions, and the emissions of pollutants.

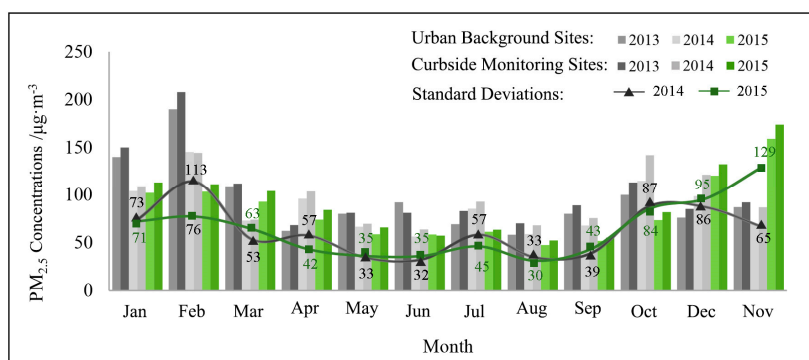


Figure 5. Monthly mean concentrations of $PM_{2.5}$ around two types of monitoring sites (Notes: Because we only can collect the monthly mean data of $PM_{2.5}$ concentrations in 2013, so the standard deviations of $PM_{2.5}$ concentrations in 2013 are missed in Figure 5.) (Source: by Authors).

3.2. LUR Model

3.2.1. Processing of Predictor Variables

We generated 25 variables in three categories and seven subcategories, to characterize the street network, land-use, and population density at different radii around each monitoring site (Table 3). The spatial analysis function of ArcGIS 10.2 was used to process these variables. Many buffer areas, which were different-sized circles centered on each monitoring site, were generated in ArcGIS 10.2 to analyze the street network, land-use, and population density around each monitoring site. The choice of the buffer sizes was based on the scales of the variables and some other studies (e.g., [41,54]).

Table 3. Classification, description, and processing methods used to generate variables in each category.

Category (N Variables)	Description	Subcategories	Buffer Radii (km)	Processing
Road length (4)	Total length (in km) of 5 road types	RD * (expressways, fast roads, arterial roads, secondary roads, branch roads)	0.5, 1, 2, 3	1. The road networks in different buffer sizes are processed by the Clip tool in ArcGIS. 2. The property sheets exported are used to analyze road lengths.
Land-use (20)	Total area (in km ²) of 5 land-use types	WT (Water), VT (vegetation), TP (transportation land), OD (other developed land), OND (other non-developed land)	0.5, 1, 2, 3	1. The land in different buffer sizes are processed by the Clip tool in ArcGIS. 2. The property sheets exported are used to analyze the area of land.
Population density (1)	Density (in persons/km ²)	PD (persons)	-	Population density of the district where each monitoring site was located has been used

* When regressing the LUR model, we found that not dividing roads into several subcategories worked better. Therefore, the *road length* variable here is not divided anymore.

3.2.2. Selection of Predictor Variables

SPSS 22.0 (International Business Machines Corporation, New York, NY, USA), a widely used software for statistical analysis in social science, was applied to analyze the correlation between PM_{2.5} concentrations and each independent variable. As shown in Table 4, out of the three types of predictor variables, the subcategories that are most relevant to the PM_{2.5} concentrations are as follows: RD₁, WT₄, VT₂, TP₂, OD₃, OND₃, and PD. According to the filtering criteria (no significant linear correlation among predictor variables, t-tests, and the contribution to R² is not below 1%), six variables were finally determined for regression: RD₁, WT₄, VT₂, TP₂, OND₃, and PD (Table 5). Except for OD₁, all of the variables highly relevant to PM_{2.5} were used for the final regression in the LUR model.

Table 4. Bivariate correlation analysis.

Number	Symbol	Variable	Pearson Correlation Coefficient (between Variables and PM _{2.5})	Pearson Correlation Coefficient (between the Most Relevant Subcategory and Others)
1	RD ₁	Road length 3 km	0.506	-
2	RD ₂	Road length 2 km	0.373	0.823
3	RD ₃	Road length 1 km	0.354	0.727
4	RD ₄	Road length 0.5 km	0.208	0.442
5	WT ₁	Water 3 km	−0.121	0.600
6	WT ₂	Water 2 km	−0.132	0.707
7	WT ₃	Water 1 km	−0.108	0.979
8	WT ₄	Water 0.5 km	−0.161	-
9	VT ₁	Vegetation 3 km	−0.679	0.948
10	VT ₂	Vegetation 2 km	−0.716	-
11	VT ₃	Vegetation 1 km	−0.701	0.967
12	VT ₄	Vegetation 0.5 km	−0.614	0.829
13	TP ₁	Transportation land 3 km	−0.250	0.521
14	TP ₂	Transportation land 2 km	−0.353	-
15	TP ₃	Transportation land 1 km	−0.199	0.882
16	TP ₄	Transportation land 0.5 km	−0.055	0.411
17	OD ₁	Other developed land 3 km	0.524	-
18	OD ₂	Other developed land 2 km	0.518	0.920
19	OD ₃	Other developed land 1 km	0.452	0.644
20	OD ₄	Other developed land 0.5 km	0.383	0.306
21	OND ₁	Other non-developed land 3 km	−0.569	-
22	OND ₂	Other non-developed land 2 km	0.318	−0.029
23	OND ₃	Other non-developed land 1 km	0.099	−0.047
24	OND ₄	Other non-developed land 0.5 km	−0.130	−0.063
25	PD	Population density	0.094	-

Note: Blue words are the subcategories that are most relevant to PM_{2.5} concentrations.

Table 5. Variables selected for final regression.

Independent Variable	Symbol
Road length 3 km	RD_1
Water 0.5 km	WT_4
Vegetation 2 km	VT_2
Transportation land 2 km	TP_2
Other non-developed land 3 km	OND_1
Population density	PD

3.2.3. Regression Result

SPSS 22.0 was used to regress $PM_{2.5}$ concentrations and the six variables selected, based on the data collected around the seventeen air-quality monitoring sites within the study area. The regression result is shown below:

$$Y_{PM_{2.5}} = 0.477 + 0.798RD_1 + 0.201WT_4 - 1.394VT_2 - 0.416TP_2 + 0.960OND_1 - 0.263PD \quad (2)$$

In Equation (2), $Y_{PM_{2.5}}$ is the annual average concentration of $PM_{2.5}$ in 2015, RD_1 is the length of roads within a buffer of 3 km, WT_4 is the water within a buffer of 0.5 km, VT_2 is the vegetation within a buffer of 2 km, TP_2 is the transportation land within a buffer of 2 km, OND_1 is the other non-developed land within a buffer of 3 km, and PD is the population density.

The determination coefficient (R^2) in this study was 0.839. Jerrett et al. (2007) [55] applied the LUR to Toronto, Ontario, Canada, and developed a model with an R^2 of 0.69. Ross et al. (2006) [45] tested the LUR model in Southern California and were able to predict 79% of the variation in NO_2 . In their review, Wu et al. (2016) [56] noted that the average R^2 of an LUR model is 0.671. Compared to these previous studies, the predictor variables selected in this study were highly relevant to $PM_{2.5}$ and fit the LUR model well.

3.3. Influence of Road Patterns on $PM_{2.5}$

3.3.1. Analysis of the Land-Use around Traffic Pollution Monitoring Sites

Five curbside monitoring sites were set along main roads to assess the influence of traffic on the air pollution in Beijing, all of which were within the study area. Figures 6 and 7 show the land-use within a buffer of 3 km around these five sites in 2015 (Table 4 shows that, only within a buffer of 3 km, is the $PM_{2.5}$ concentration most correlated with road patterns. Therefore, the 3 km buffer radii was selected here, as well as in Figures 8 and 9.).

From the two figures above, it can be seen that there are some similarities in the land-use pattern around the five curbside monitoring sites, such as similar grid layouts of the land-use divided by roads and similar land-use structures, with *other developed land* being the first, followed by *vegetation*, *water*, *transportation land*, and *other non-developed land*. When considering the percentage of *vegetation*, monitoring site 5 has a significantly higher percentage than the others, while monitoring site 3 has a significantly lower value than the others. As for the percentage of *other non-developed land*, monitoring site 5 has the lowest percentage, while monitoring site 3 has the highest value. From Equation (2), it can be seen that the three variables most relevant to $PM_{2.5}$ concentrations are *vegetation*, *other non-developed land*, and *road length*. Based on the controlling variables method, monitoring sites with a similar land-use structure should be selected to analyze the influence of road patterns on $PM_{2.5}$, because under this circumstance, the impact of land-use on $PM_{2.5}$ concentrations can be ignored. Therefore, monitoring sites 3 and 5, whose proportions of *vegetation* and *other non-developed land* show large differences, were excluded, while sites 1, 2, and 4 were selected for the study. By comparing the road patterns and the $PM_{2.5}$ distribution of the selected monitoring sites, the relationship between the two was determined.



Figure 6. Land-use layout around the curbside monitoring sites in 2015 (Source: Basic data from Beijing Municipal Institute of City Planning & Design and Google Earth, modified by authors).

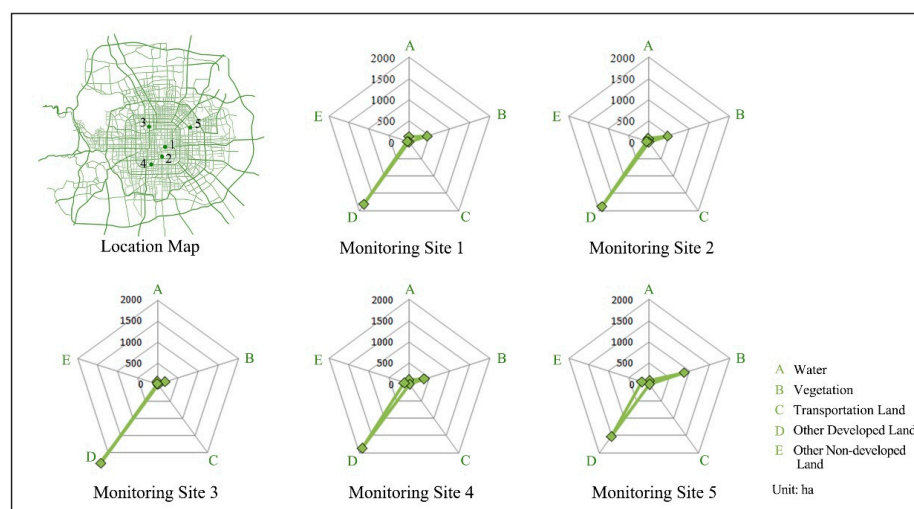


Figure 7. Land-use structure around the curbside monitoring sites in 2015 (Source: by Authors).

3.3.2. Link between Road Patterns and PM_{2.5} Concentrations

(1) Comparison of road patterns around the curbside monitoring sites

Monitoring site 1 was located at the East Avenue of Qianmen, near Tian'anmen Square and East 2nd Ring Road. The surrounding street network shows a relatively uniform grid pattern, with arterial roads forming the skeletal structure of the road, while the branch and secondary roads weaved through them. The density of this road network reaches 23.3 km/km². Monitoring site 2 lies along the Inner Avenue of Yongding Gate, near the Temple of Heaven and the North 2nd Ring Road. Branch roads and arterial roads are the major components of the street network near this site. Moreover, this network shows some differences between the southern and the northern areas: the road density in the south is lower than that in the north; fast roads and arterial roads constitute the skeleton of the network in the south, while arterial roads and secondary roads constitute the skeleton of the network in the north.

The density of the whole road network around monitoring site 2 reaches 22.2 km/km^2 . Monitoring site 3 is located near the Southwest 3rd Ring Road and Jingkai Expressway. The surrounding street network shows a relatively uniform and low-density grid pattern, and the proportion of fast roads is higher than the other two monitoring sites. There are also some small differences between the south and the north, such as the arterial roads and branch roads, which are mainly concentrated in the north, and the expressway, which only appears in the south. The density of the entire road network around monitoring site 3 is 22.2 km/km^2 .

There are significant differences in the road network of the three monitoring sites (Figures 8 and 9). When considering the road density, the following relationship can be seen: monitoring site 1 > monitoring site 2 > monitoring site 3. With regard to the road grade structure, both monitoring sites 1 and 2 are mainly dominated by branch roads and secondary roads, while monitoring site 4 features a relatively uniform network structure, with an expressway also running around it. As for the layout of the road network, the network near monitoring site 1 shows a relatively high-density grid pattern, with the main streets forming a fishbone shape, while the network near monitoring sites 2 and 4 shows a relatively low-density grid pattern, with the road in the north being denser than that in the south.

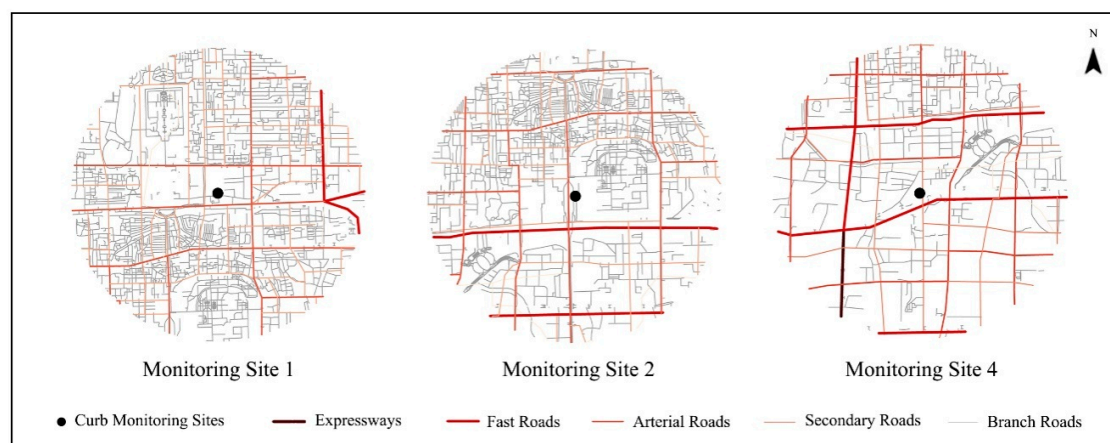


Figure 8. Road network layout around curbside monitoring sites in 2015 (Source: Basic data from Beijing Municipal Institute of City Planning & Design and Google Earth, modified by authors).

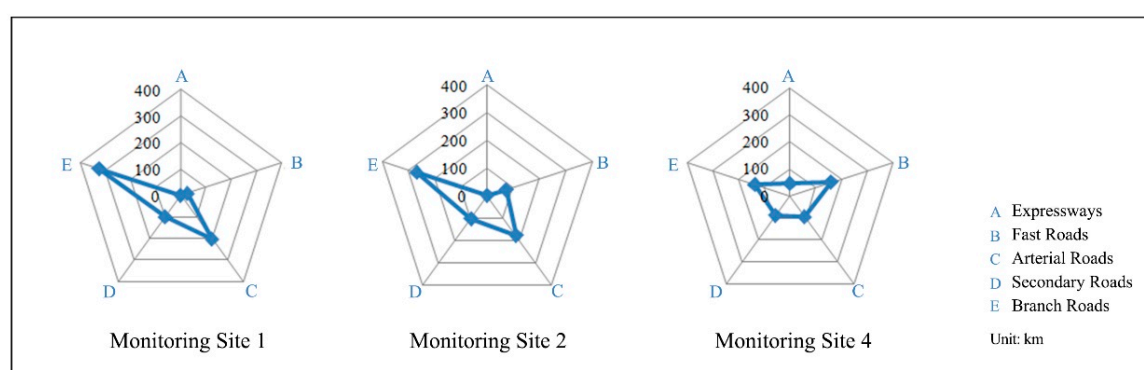


Figure 9. Road network structure around the curbside monitoring sites in 2015 (Source: by Authors).

(2) Comparison of $\text{PM}_{2.5}$ concentrations around traffic pollution monitoring stations

There are some differences in the distribution of $\text{PM}_{2.5}$ around the three monitoring sites (Table 6). These differences among the concentrations look small, but they are quite important and meaningful, because even a small change in $\text{PM}_{2.5}$ concentrations could indicate a big change in the total emission of $\text{PM}_{2.5}$. Furthermore, some research has highlighted that slight variations in $\text{PM}_{2.5}$ concentrations have

a great influence on a human's health. For example, the government of London released a report by Dr. Brian G Miller in 2010, which said that every $1 \mu\text{g}/\text{m}^3$ permanent increase in $\text{PM}_{2.5}$ concentrations is associated with a mean reduction in life expectancy of three weeks [57]. When focusing on the annual mean and median of $\text{PM}_{2.5}$ in 2015, the following pattern emerges: monitoring site 4 > monitoring site 1 > monitoring site 2. With regard to the amplitude of annual variation, the following relationship is recorded: monitoring site 1 \approx monitoring site 4 > monitoring site 2. As for the upper and lower limits of the 95% confidence interval: monitoring site 4 > monitoring site 1 > monitoring site 2. The seasonal mean, except for the abnormally high level of monitoring site 2 in winter, the other seasons were almost aligned as: monitoring site 4 > monitoring site 1 > monitoring site 2. In summary, when considering the three monitoring sites, the $\text{PM}_{2.5}$ concentration of site 4 was the highest, followed by site 1, and site 2 presented the lowest values. The fluctuations demonstrated at sites 4 and 1 were significantly higher than that of site 2.

Table 6. Comparison of $\text{PM}_{2.5}$ concentrations.

Monitoring Site	Annual Variation in 2015				Seasonal Mean (µg/m³)				
	Mean (µg/m³)	Median (µg/m³)	Bound of 95% Confidence Interval		Standard Deviation	Winter	Spring	Summer	Autumn
No. 1	92.9	66.5	83.2	101.1	85.1	101.0	89.4	60.5	89.5
No. 2	89.9	65.0	81.3	98.4	81.3	104.4	79.7	57.2	88.9
No. 4	96.1	71.5	87.3	105.0	84.5	108.8	86.7	62.6	93.2

(3) Link between road patterns and $\text{PM}_{2.5}$

From Equation (2), it can be seen that the three variables which are apparently relevant to $\text{PM}_{2.5}$ concentrations are *vegetation*, *other non-developed land*, and *road length*. According to the analysis in the Section 3.3.1 "Analysis of the land-use around traffic pollution monitoring sites", it is clear that the land-use structures of monitoring sites 1, 2, and 4 are similar. Therefore, we can conclude that the differences in $\text{PM}_{2.5}$ concentrations between these three sites are mainly caused by the differences in road patterns, based on the controlling variables method. Under this circumstance, by comparing the road patterns and the $\text{PM}_{2.5}$ distribution of the selected monitoring sites, the relationship between the two can be concluded.

First, both the grade of road and the road density influence $\text{PM}_{2.5}$ concentrations. Under the same traffic carrying capacity, the high-grade road network, which has a low density, will be more likely to improve the concentration of $\text{PM}_{2.5}$ than the low-grade road network, which has a high density. This means that the layout of "a tight network of streets and small blocks" is superior to the layout of "a sparse network of streets and big blocks", from an environmental and sustainable point of view (by comparing monitoring sites 1, 2, and 4). The layout of "a tight network of streets and small blocks" originates from the city-plan idea of new urbanism, which is used to solve the problem of low-density road networks, serious block segmentation, high transportation energy consumption, traffic jams, etc., caused by the traditional mode of urban planning. With regard to $\text{PM}_{2.5}$, this paper provides a more convincing evidence for the reasonability of the layout of "a tight network of streets and small blocks".

Second, the grade system of urban roads impacts the rationality of the road patterns, and the high percentage of branch roads and secondary roads decreases $\text{PM}_{2.5}$ concentrations (by comparing monitoring sites 1, 2, and 4). Without secondary roads, the connection between arterial roads and the place where traffic originates, will be insufficient. Without branch roads, secondary roads will bear the function of branch roads, which will make it more difficult for the secondary roads to maintain their own function, eventually leading to the disorganization of the entire road system. All of the above situations will result in the overlap of different speeds of traffic flows, and the overload of several accessible and convenient roads, which can hinder urban traffic evacuation. The percentage of low and middle grade roads in developed countries, such as America and Japan, could reach 80%, with the distribution proportion of roads from low-grade to high-grade being like a pyramid.

Third, keeping traffic nodes unimpeded will significantly reduce the concentration of $PM_{2.5}$ (by comparing monitoring sites 1 and 2). Unimpeded traffic nodes not only improve the operating efficiency of the whole road network, but also reduce the obstruction to the wind field, which accelerates the diffusion of $PM_{2.5}$. The planning of road directions should also take into consideration the local prevailing wind direction. The street canyons, which are parallel to the wind, could be helpful for the diffusion of air pollutants through the transport effect of wind. The air pollutants in the street canyons that are vertical to the direction of wind will diffuse less rapidly.

4. Conclusions and Discussion

With the fast development of motorized transport, the air pollution caused by traffic has been a major source of pollutants in modern cities. Much research has been performed on $PM_{2.5}$, but the study of the correlation between road patterns and $PM_{2.5}$ is a relatively new field. One major limitation of this study is the fact that there are only five curbside monitoring sites. The limited samples make it difficult to quantitatively research how the density, grade, and form of road network, affect $PM_{2.5}$ concentrations. Under this circumstance, we chose a control variate method to perform our research, which inevitably results in some subjective errors. Another limitation is that this case study relates to the road patterns and $PM_{2.5}$ in Beijing alone. Hence, more research on various types of cities should be undertaken, to enrich the findings and make them more universal. Despite these limitations, we believe that this research still offers an important insight into the relationship between road patterns and $PM_{2.5}$. The main conclusions are as follows.

(1) Do road patterns significantly affect $PM_{2.5}$ concentrations?

First, the LUR model developed in this paper can explain 83.9% of the variation in $PM_{2.5}$ levels, which shows that the selected predictor variables are highly relevant to $PM_{2.5}$, and that this model is a good fit for the Beijing. Second, from highly relevant to $PM_{2.5}$, to weakly relevant to $PM_{2.5}$, the variables are, *vegetation, other non-developed land, road length, transportation land, population density, and water*. Among these variables, the regression coefficient of *road length* is up to 0.798, which is significantly higher than *water, population density, and transportation land*, which shows that road patterns have an obvious effect on $PM_{2.5}$ concentrations. Third, the regression coefficient of road patterns is positive, indicating that traffic improves the concentration of $PM_{2.5}$, consistent with daily experiences. Fourthly, according to Table 4, we can conclude that the correlation between $PM_{2.5}$ and road patterns increases with the increasing of a buffer zone.

(2) How do road patterns affect $PM_{2.5}$ concentrations?

First, both the grade of road and the road density influence $PM_{2.5}$ concentrations. Under the same traffic carrying capacity, the high-grade road network, that has a low density, will be more likely to improve $PM_{2.5}$ concentrations than the low-grade road network, that has a high density. This means that the layout of “a tight network of streets and small blocks” is superior to the layout of “a sparse network of streets and big blocks”. Second, the grade proportion of urban roads impacts the rationality of the road patterns, and a high percentage of branch roads and secondary roads could decrease $PM_{2.5}$ concentrations. Third, keeping traffic nodes unimpeded can significantly reduce $PM_{2.5}$ concentrations.

Acknowledgments: This work was supported by the Sino-German Center (NSFC and DFG, Grant No. GZ1201).

Author Contributions: Fang Wang was in charge of this research. She contributed to data processing and drafting the manuscript; Yaoyao Peng contributed to data collection, data analysis, and paper revision; Chunyan Jiang contributed to data analysis and paper revision. All authors read and approved the final manuscript.

Conflicts of Interest: The authors declare no conflict of interest.

References

1. Sun, Y.; Zhuang, G.; Wang, Y.; Han, L.; Guo, J.; Dan, M.; Zhang, W.J.; Wang, Z.F.; Hao, Z.P. The air-borne particulate pollution in Beijing—Concentration, composition, distribution and sources. *Atmos. Environ.* **2004**, *38*, 5991–6004. [[CrossRef](#)]
2. Xu, H.; Bi, X.H.; Zheng, W.W.; Wu, J.H.; Feng, Y.C. Particulate matter mass and chemical component concentrations over four Chinese cities along the western Pacific coast. *Environ. Sci. Pollut. Res.* **2015**, *22*, 1940–1953. [[CrossRef](#)] [[PubMed](#)]
3. Li, S.; Zhu, L.; Shi, T.M.; Wang, W. The counter measures of urban street planning based on the pollution prevention of inhalant particle. *Urban Dev. Stud.* **2014**, *21*, 42–45. (In Chinese)
4. Weng, Q.H.; Yang, S.H. Urban air pollution patterns, land use, and thermal landscape: An examination of the linkage using GIS. *Environ. Monit. Assess.* **2006**, *117*, 463–489. [[CrossRef](#)] [[PubMed](#)]
5. Schweitzer, L.; Zhou, J. Neighborhood air quality, respiratory health, and vulnerable populations in compact and sprawled regions. *J. Am. Plan. Assoc.* **2010**, *76*, 363–371. [[CrossRef](#)]
6. Li, X.Y.; Zhao, S.T.; Li, Y.M.; Guo, J.; Li, W. Subduction effect of urban arteries green space on atmospheric concentration of PM_{2.5} in Beijing. *Ecol. Environ. Sci.* **2014**, *23*, 615–621. (In Chinese)
7. Levy, J.I.; Bennett, D.H.; Melly, S.J.; Spengler, J.D. Influence of road patterns on particulate matter and polycyclic aromatic hydrocarbon concentrations in Roxbury, Massachusetts. *J. Expo. Sci. Environ. Epidemiol.* **2003**, *13*, 364–371. [[CrossRef](#)] [[PubMed](#)]
8. Chan, L.Y.; Kwok, W.S.; Lee, S.C.; Chan, C.Y. Spatial variation of mass concentration of roadside suspended particulate matter in metropolitan Hong Kong. *Atmos. Environ.* **2001**, *35*, 3167–3176. [[CrossRef](#)]
9. Li, X.Y.; Li, Y.M.; Zhao, S.T.; Guo, J. Influence of urban green spaces on the concentration of PM_{2.5}. In *Beijing Botanical Garden Afforestation and Livable City Construction*, Proceedings of the Beijing Institute of Landscape architecture Academic Forum 2012, Beijing, China, 22–23 November 2012; pp. 17–20. (In Chinese)
10. Chow, J.C.; Watson, J.G.; Frazier, C.A.; Egami, R.T.; Goodrich, A.; Ralph, C. Spatial and temporal source contributions to PM₁₀ and PM_{2.5} in Reno, NV. In *PM-10: Implementation of Standards: Transactions, Proceedings of the APCA/EPA International Speciality Conference*, San Francisco, CA, USA, 22–26 February 1988; Mathal, C.V., Stonefield, D.H., Eds.; APCA: Pittsburgh, PA, USA, 1988; pp. 439–457.
11. Japar, S.M. Motor vehicles and particle air pollution: An overview. In *Particulate Matter: Health and Regulatory Issues VIP-49*, Proceedings of the Air and Waste Management Association International Specialty Conference, Pittsburgh, PA, USA, 8–12 November 1993; pp. 577–598.
12. Gertler, A.W.; Gillies, J.A.; Pierson, W.R. An assessment of the mobile source contribution to PM₁₀ and PM_{2.5} in the United States. *Water Air Soil Pollut.* **2000**, *123*, 203–214. [[CrossRef](#)]
13. Wang, J.S.; Chan, T.L.; Ning, Z.; Leung, C.W.; Cheung, C.S.; Hung, W.T. Roadside measurement and prediction of CO and PM_{2.5} dispersion from on-road vehicles in Hong Kong. *Transp. Res. D Transp. Environ.* **2006**, *11*, 242–249. [[CrossRef](#)]
14. Myung, C.L.; Park, S. Exhaust nanoparticle emissions from internal combustion engines: A review. *Int. J. Automot. Technol.* **2012**, *13*, 9–22. [[CrossRef](#)]
15. Zheng, X.; Wu, Y.; Jiang, J.K.; Zhang, S.J.; Liu, H.; Song, S.J.; Li, Z.H.; Fan, X.X.; Fu, L.X.; Hao, J.M. Characteristics of on-road diesel vehicles: Black carbon emissions in Chinese Cities based on portable emissions measurement. *Environ. Sci. Technol.* **2015**, *49*, 13492–13500. [[CrossRef](#)] [[PubMed](#)]
16. Lau, C.F.; Rakowska, A.; Townsend, T.; Brimblecombe, P.; Chan, T.L.; Yam, Y.S.; Mocnik, C.; Ning, Z. Evaluation of diesel fleet emissions and control policies from plume chasing measurements of on-road vehicles. *Atmos. Environ.* **2015**, *122*, 171–182. [[CrossRef](#)]
17. Ministry of Environmental Protection of the People's Republic of China. *China Vehicle Emission Control Annual Report 2016*; Ministry of Environmental Protection of the People's Republic of China: Beijing, China, 2016.
18. Choi, K.; Kim, J.; Ko, A.; Myung, C.L.; Park, S.; Lee, J. Size-resolved engine exhaust aerosol characteristics in a metal foam particulate filter for GDI light-duty vehicle. *J. Aerosol Sci.* **2013**, *57*, 1–13. [[CrossRef](#)]

19. Gillies, J.A.; Gertler, A.W.; Sagebiel, J.C.; Dippel, N.W. On-road particulate matter (PM_{2.5} and PM₁₀) emissions in the Sepulveda Tunnel, Los Angeles, California. *Environ. Sci. Technol.* **2001**, *35*, 1054–1063. [[CrossRef](#)] [[PubMed](#)]
20. Aldabe, J.; Elustondo, D.; Santamaría, C.; Lasheras, E.; Pandolfi, M.; Alastuey, A.; Querol, X.; Santamaria, J.M. Chemical characterisation and source apportionment of PM_{2.5} and PM₁₀ at rural, urban and traffic sites in Navarra (North of Spain). *Atmos. Res.* **2011**, *102*, 191–205. [[CrossRef](#)]
21. Perugu, H.; Wei, H.; Yao, Z. Integrated data-driven modeling to estimate PM_{2.5} pollution from heavy-duty truck transportation activity over metropolitan area. *Transp. Res. D Transp. Environ.* **2016**, *46*, 114–127. [[CrossRef](#)]
22. Buckeridge, D.L.; Glazier, R.; Harvey, B.J.; Escobar, M.; Amrhein, C.; Frank, J. Effect of motor vehicle emissions on respiratory health in an urban area. *Environ. Health Perspect.* **2002**, *110*, 293–300. [[CrossRef](#)] [[PubMed](#)]
23. Fann, N.; Lamson, A.D.; Anenberg, S.C.; Wesson, K.; Risley, D.; Hubbell, B.J. Estimating the national public health burden associated with exposure to ambient PM_{2.5} and ozone. *Risk Anal.* **2012**, *32*, 81–95. [[CrossRef](#)] [[PubMed](#)]
24. Ying, Z.; Xu, X.; Bai, Y.; Zhong, J.; Chen, M.; Liang, Y.; Zhao, J.; Liu, D.; Morishita, M.; Sun, O.; et al. Long-term exposure to concentrated ambient PM_{2.5} increases mouse blood pressure through abnormal activation of the sympathetic nervous system: A role for hypothalamic inflammation. *Environ. Health Perspect.* **2014**, *122*, 79–86. [[CrossRef](#)] [[PubMed](#)]
25. Panis, L.I.; Beckx, C.; Broekx, S.; De Vlieger, I.; Schrooten, L.; Degraeuwe, B.; Pelkmans, L. PM, NO_x and CO₂ emission reductions from speed management policies in Europe. *Transp. Policy* **2011**, *18*, 32–37. [[CrossRef](#)]
26. Xu, B.; Yu, X.; Gu, H.; Miao, B.; Wang, M.; Huang, H. Commuters' exposure to PM_{2.5} and CO₂ in metro carriages of Shanghai metro system. *Transp. Res. D Transp. Environ.* **2016**, *47*, 162–170. [[CrossRef](#)]
27. Maddison, D.; Mourato, S. Valuing different road options for Stonehenge. *Conserv. Manag. Archaeol. Sites* **2001**, *4*, 203–212. [[CrossRef](#)]
28. Xie, X.M.; Huang, Z.; Wang, J.S. The impact of urban street layout on local atmospheric environment. *Build. Environ.* **2006**, *41*, 1352–1363.
29. Brook, J.R.; Dann, T.F.; Burnett, R.T. The relationship among TSP, PM₁₀, PM_{2.5}, and inorganic constituents of atmospheric particulate matter at multiple Canadian locations. *J. Air Waste Manag. Assoc.* **1997**, *47*, 2–19. [[CrossRef](#)]
30. Lee, S.J.; Serre, M.L.; van Donkelaar, A.; Martin, R.V.; Burnett, R.T.; Jerrett, M. Comparison of geostatistical interpolation and remote sensing techniques for estimating long-term exposure to ambient PM_{2.5} concentrations across the continental United States. *Environ. Health Perspect.* **2012**, *120*, 1727–1732. [[CrossRef](#)] [[PubMed](#)]
31. Hankey, S.; Marshall, J.D. Land use regression models of on-road particulate air pollution (particle number, black carbon, PM_{2.5}, particle size) using mobile monitoring. *Environ. Sci. Technol.* **2015**, *49*, 9194–9202. [[CrossRef](#)] [[PubMed](#)]
32. Chang, S.Y.; Vizuete, W.; Valencia, A.; Naess, B.; Isakov, V.; Palma, T.; Breen, M.; Arunachalam, S. A modeling framework for characterizing near-road air pollutant concentration at community scales. *Sci. Total Environ.* **2015**, *538*, 905–921. [[CrossRef](#)] [[PubMed](#)]
33. Beckerman, B.S.; Jerrett, M.; Serre, M.; Martin, R.V.; Lee, S.J.; van Donkelaar, A.; Ross, Z.; Su, J.; Burnett, R. A hybrid approach to estimating national scale spatiotemporal variability of PM_{2.5} in the contiguous United States. *Environ. Sci. Technol.* **2013**, *47*, 7233–7241.
34. De Hoogh, K.; Korek, M.; Vienneau, D.; Keuken, M.; Kukkonen, J.; Nieuwenhuijsen, M.J.; Pradas, M.C. Comparing land use regression and dispersion modelling to assess residential exposure to ambient air pollution for epidemiological studies. *Environ. Int.* **2014**, *73*, 382–392. [[CrossRef](#)] [[PubMed](#)]
35. Hoek, G.; Beelen, R.; De Hoogh, K.; Vienneau, D.; Gulliver, J.; Fischer, P.; Briggs, D. A review of land-use regression models to assess spatial variation of outdoor air pollution. *Atmos. Environ.* **2008**, *42*, 7561–7578. [[CrossRef](#)]

36. Lee, J.H.; Wu, C.F.; Hoek, G.; de Hoogh, K.; Beelen, R.; Brunekreef, B.; Chan, C.C. LUR models for particulate matters in the Taipei metropolis with high densities of roads and strong activities of industry, commerce and construction. *Sci. Total Environ.* **2015**, *514*, 178–184. [[CrossRef](#)] [[PubMed](#)]
37. Henderson, S.B.; Beckerman, B.; Jerrett, M.; Brauer, M. Application of land use regression to estimate long-term concentrations of traffic-related nitrogen oxides and fine particulate matter. *Environ. Sci. Technol.* **2007**, *41*, 2422–2428. [[CrossRef](#)] [[PubMed](#)]
38. Sahsuvaroglu, T.; Arain, A.; Kanaroglou, P.; Finkelstein, N.; Newbold, B.; Jerrett, M.; Beckerman, B.; Brook, J.; Finkelstein, M.; Gilbert, N.L. A land use regression model for predicting ambient concentrations of nitrogen dioxide in Hamilton, Ontario, Canada. *J. Air Waste Manag. Assoc.* **2006**, *56*, 1059–1069. [[CrossRef](#)] [[PubMed](#)]
39. Thomas, D.; Stram, D.; Dwyer, J. Exposure measurement error: Influence on exposure-disease relationships and methods of correction. *Annu. Rev. Public Health* **1993**, *14*, 69–93. [[CrossRef](#)] [[PubMed](#)]
40. Briggs, D.J.; Collins, S.; Elliott, P.; Fischer, P.; Kingham, S.; Lebret, E.; Pyl, K.; van Reeuwijk, H.; Smallbone, K.; van der Veen, A. Mapping urban air pollution using GIS: A regression-based approach. *Int. J. Geogr. Inf. Sci.* **1997**, *11*, 699–718. [[CrossRef](#)]
41. Ross, Z.; Jerrett, M.; Ito, K.; Tempalski, B.; Thurston, G.D. A land use regression for predicting fine particulate matter concentrations in the New York City region. *Atmos. Environ.* **2007**, *41*, 2255–2269. [[CrossRef](#)]
42. Lebret, E.; Briggs, D.; Van Reeuwijk, H.; Fischer, P.; Smallbone, K.; Harssema, H.; Kriz, B.; Gorynski, P.; Elliott, P. Small area variations in ambient NO₂ concentrations in four European areas. *Atmos. Environ.* **2000**, *34*, 177–185. [[CrossRef](#)]
43. Brauer, M.; Hoek, G.; van Vliet, P.; Meliefste, K.; Fischer, P.; Smallbone, K.; Harssema, H.; Kriz, B.; Gorynski, P.; Elliott, P. Estimating long-term average particulate air pollution concentrations: Application of traffic indicators and geographic information systems. *Epidemiology* **2003**, *14*, 228–239. [[CrossRef](#)] [[PubMed](#)]
44. Gilbert, N.L.; Goldberg, M.S.; Beckerman, B.; Brook, J.R.; Jerrett, M. Assessing spatial variability of ambient nitrogen dioxide in Montreal, Canada, with a land-use regression model. *J. Air Waste Manag. Assoc.* **2005**, *55*, 1059–1063. [[CrossRef](#)] [[PubMed](#)]
45. Ross, Z.; English, P.B.; Scalf, R.; Gunier, R.; Smorodinsky, S.; Wall, S.; Jerrett, M. Nitrogen dioxide prediction in Southern California using land use regression modeling: Potential for environmental health analyses. *J. Expo. Sci. Environ. Epidemiol.* **2006**, *16*, 106–114. [[CrossRef](#)] [[PubMed](#)]
46. Beelen, R.; Hoek, G.; Vienneau, D.; Eeftens, M.; Dimakopoulou, K.; Pedeli, X.; Eriksen, K.T. Development of NO₂ and NO_x land use regression models for estimating air pollution exposure in 36 study areas in Europe—The ESCAPE project. *Atmos. Environ.* **2013**, *72*, 10–23. [[CrossRef](#)]
47. Wheeler, A.J.; Smith-Doiron, M.; Xu, X.; Gilbert, N.L.; Brook, J.R. Intra-urban variability of air pollution in Windsor, Ontario—Measurement and modeling for human exposure assessment. *Environ. Res.* **2008**, *106*, 7–16. [[CrossRef](#)] [[PubMed](#)]
48. Lee, J.H.; Wu, C.F.; Hoek, G.; de Hoogh, K.; Beelen, R.; Brunekreef, B.; Chan, C.C. Land use regression models for estimating individual NO_x and NO₂ exposures in a metropolis with a high density of traffic roads and population. *Sci. Total Environ.* **2014**, *472*, 1163–1171. [[CrossRef](#)] [[PubMed](#)]
49. The people's Government of Beijing City. *Master Planning of Beijing (2004–2020)*; Beijing City Planning & Construction Review: Beijing, China, 2005; pp. 5–51.
50. Beijing Institute of Surveying and Mapping. *Beijing Traffic Tourism Map*; Sinomap Press: Beijing, China, 2015.
51. Wu, J.S.; Liao, X.; Peng, J.; Huang, X.L. Simulation and Influencing Factors of Spatial Distribution of PM_{2.5} Concentrations in Chongqing. *Environ. Sci.* **2015**, *36*, 759–767. (In Chinese)
52. Beijing Statistical Bureau. *Beijing Statistical Yearbook*; China Statistics Press: Beijing, China, 2015; p. 65.
53. Wang, Y.S.; Yao, L.; Wang, L.L.; Liu, Z.R.; Ji, D.S.; Tang, G.Q.; Zhang, J.K.; Sun, Y.; Hu, B.; Xin, J.Y. Mechanism for the formation of the January 2013 heavy haze pollution episode over central and eastern China. *Sci. China Earth Sci.* **2014**, *44*, 15–26. (In Chinese) [[CrossRef](#)]
54. Wang, M.; Beelen, R.; Bellander, T.; Birk, M.; Cesaroni, G.; Cirach, M.; Cyrys, J.; de Hoogh, K.; Declercq, C.; Dimakopoulou, K.; et al. Performance of multi-city land use regression models for nitrogen dioxide and fine particles. *Environ. Health Perspect.* **2014**, *122*, 843–849. [[CrossRef](#)] [[PubMed](#)]
55. Jerrett, M.; Arain, M.A.; Kanaroglou, P.; Beckerman, B.; Crouse, D.; Gilbert, N.L.; Brook, J.R.; Finkelstein, N.; Finkelstein, M.M. Modeling the intraurban variability of ambient traffic pollution in Toronto, Canada. *J. Toxicol. Environ. Health A* **2007**, *70*, 200–212. [[CrossRef](#)] [[PubMed](#)]

56. Wu, J.S.; Xie, W.D.; Li, J.C. Application of Land-use Regression Models in Spatial-temporal Differentiation of Air Pollution. *Environ. Sci.* **2016**, *37*, 413–419. (In Chinese)
57. Miller, B. Report on Estimation of Mortality Impacts of Particulate Air Pollution in London. Consulting Report P951-001. 2010. Available online: http://www.aef.org.uk/uploads/IomReport_1.pdf (accessed on 6 February 2017).



© 2017 by the authors; licensee MDPI, Basel, Switzerland. This article is an open access article distributed under the terms and conditions of the Creative Commons Attribution (CC BY) license (<http://creativecommons.org/licenses/by/4.0/>).